Nuclear and Emerging Technologies for Space, American Nuclear Society Topical Meeting
Richland, WA, February 25 – February 28, 2019, available online at http://anstd.ans.org/

DESIGN OPTIMIZATION STUDIES FOR NPO2 TARGETS IRRADIATED IN THE HIGH FLUX ISOTOPE REACTOR[1]

C. R. Daily[1] and J. L. McDuffee[1]

[1]*Oak Ridge National Laboratory, P.O. Box 2008, Oak Ridge, TN, 37831-6170, USA, dailycr@ornl.gov*

Efforts to re-establish a domestic ^{238}Pu production capability in support of National Aeronautics and Space Administration (NASA) mission objectives are ongoing throughout the US Department of Energy (DOE) complex. Design and optimization studies of ^{237}Np-bearing targets are underway at Oak Ridge National Laboratory (ORNL). It is anticipated that targets will be irradiated in ORNL's High Flux Isotope Reactor (HFIR) and in the Advanced Test Reactor at Idaho National Laboratory. A variety of target materials, containments, arrangements, and irradiation histories have been analyzed, and the results indicate that a sufficient quantity of ^{238}Pu can be produced in HFIR to fulfill NASA's current mission objectives. This paper focuses on the design and optimization of new target configurations containing pellets that are (1) 92% ± 2% of the theoretical density (TD) of NpO_2, (2) loaded into pins of cladding materials that can be handled as solid waste following post-irradiation ^{238}Pu recovery operations, (3) irradiated in various vertical experiment facility (VXF) locations in the HFIR permanent beryllium reflector, and (4) rotated within and/or moved to another VXF location following each HFIR operational cycle to maximize ^{238}Pu production and minimize peak heat generation rates.

I. INTRODUCTION

To support National Aeronautics and Space Administration (NASA) mission requirements, Oak Ridge National Laboratory (ORNL) is participating in a technology demonstration project to re-establish a domestic supply chain of PuO_2 through the irradiation of $^{237}NpO_2$-bearing targets. Target irradiation is planned at the High Flux Isotope Reactor (HFIR), which is located at ORNL, and the Advanced Test Reactor, which is located at Idaho National Laboratory.[1]

This paper summarizes the design studies performed on targets containing $^{237}NpO_2$ formed into pellets that are in the range of 92% ± 2% of theoretical density (TD). Results from these studies indicate that NASA mission requirements for ~1.5 kg/yr of PuO_2, with a minimum quality (ratio of ^{238}Pu mass to total mass of all Pu isotopes) of 85% can be met through HFIR irradiations. Because of the increased initial $^{237}NpO_2$ mass relative to previous target designs containing cermet pellets[2] (70 vol.% aluminum, 20% $^{237}NpO_2$, and 10% void), the desired annual quantity of PuO_2 can be produced with fewer targets.

I.A. High Flux Isotope Reactor

HFIR is a US Department of Energy (DOE) user facility which was originally designed in the late 1950s and early 1960s for the sole purpose of producing trans-plutonium isotopes.[3] Operations in support of this mission began in 1966. Today, the mission-space of HFIR includes thermal neutron scattering experiments, numerous isotope production campaigns (including ^{238}Pu), and materials irradiation and testing initiatives.

HFIR is a light-water–cooled, light-water–moderated, beryllium-reflected flux-trap type reactor that operates at a steady-state power of 85 MW. A typical operational cycle lasts between 24 and 26 days, producing a peak thermal flux of ~2.5×10^{15} n/cm^2-s in the inner flux trap (IFT) region. For the past few years, an operational schedule of 7 cycles per year has been achieved.

The HFIR core consists of inner and outer fuel elements. The inner fuel element contains 171 involute-shaped fuel plates, and the outer fuel element contains 369. A total of ~9.4 kg of ^{235}U in the form of highly enriched uranium is contained in the fuel plates. The core surrounds the IFT and is surrounded by two cylindrical control elements (CEs) and a reflector assembly consisting of the removable beryllium (RB), semi-permanent beryllium, and permanent beryllium (PB) zones. The IFT and each of the reflector zones contain irradiation facilities as depicted in Figure 1.

Four horizontal beam (HB) tubes that provide thermal or cold neutrons for various scattering experiments penetrate the PB. The beam tubes are labeled as HB-1 through HB-4, as shown in Figure 1. The IFT contains six peripheral target positions (PTPs), 30 target rods (TRs), and 1 hydraulic tube (HT). As shown in the inset to Figure 1, the PTPs are shown in orange, the TRs are depicted in white, and the HT is shown in red. The RB, which is depicted in purple in Figure 1, contains 8 large (~2.33 cm diameter) and 4 small (0.635 cm diameter) irradiation

facilities. The PB, which is depicted in green in Figure 1, contains 22 vertical experiment facilities (VXF). The 22 VXFs consist of 11 inner-small (ISVXF), 5 outer-small (OSVXF), and 6 outer-large (OLVXF) positions. The ISVXFs and OSVXFs are ~2.01 cm in diameter, while the OLVXFs have a diameter of ~3.60 cm. The centerlines of the ISVXF, OSVXF, and OLVXF positions are ~39.21 cm, 44.05 cm, and 46.28 cm from the centerline of the core, respectively.

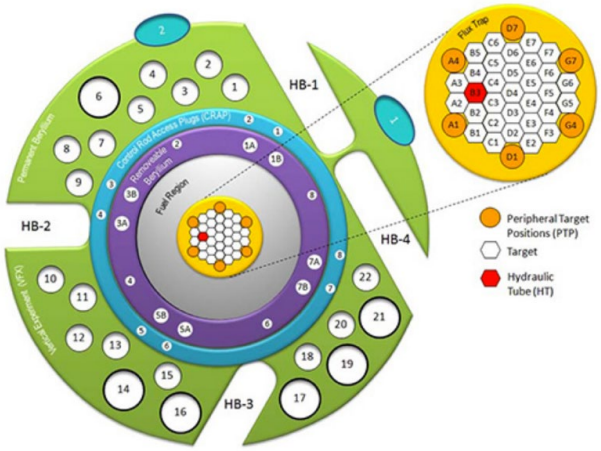

Fig. 1. HFIR core and target schematic <https://neutrons.ornl.gov/suites/in-vessel-irradiation>.

I.B. Production and Usage of $^{238}PuO_2$.

The predominant production path for ^{238}Pu is through neutron irradiation of ^{237}Np. The neutron capture (n,γ) reaction in ^{237}Np produces ^{238}Np, which subsequently undergoes β^- decay with a 2.12-day half-life to yield ^{238}Pu. Competing with this production path is the loss of ^{238}Np atoms through fission before they decay to ^{238}Pu. Additionally, some of the ^{238}Pu that is produced is lost through various absorptive reactions such as (n,γ) and (n,2n). This leads to the buildup of other Pu isotopes. These production and loss processes are depicted in Figure 2. Once irradiation ends, the Pu can be extracted from the NpO_2-bearing targets. ^{238}Pu emits high-energy alpha particles with a long (~87.7-year) half-life, making it a reliable, long-lasting heat source to power radioisotope thermoelectric generators (RTGs) in the form of PuO_2. These RTGs are used to provide a reliable source of electricity for NASA's deep space and planetary missions.

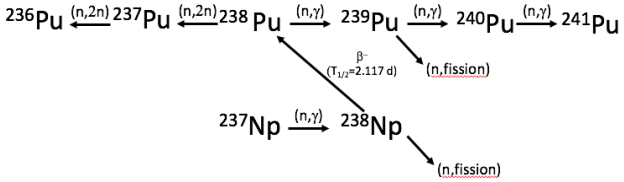

Fig. 2. Schematic representation of ^{238}Pu production and loss processes.

II. COMPUTATIONAL METHODS

Multicycle depletion analyses were performed for a variety of target designs. These analyses used the MCNP[4] Monte-Carlo transport code, the ADVANTG[5] variance reduction code, and the ORIGEN[6] point depletion and decay code to generate time-dependent heat generation rates and isotopic inventories, including fission gas quantities.

A set of Python scripts that were originally written for previous analyses[2,7] and then modified as needed for a variety of different analyses were tailored to the current analysis and used to couple the MCNP and ORIGEN codes. In this process, an MCNP model with beginning-of-cycle (BOC) core and CE isotopic number densities and CE positions,[7] as well as fresh target inventories, was used to generate spatially dependent fluxes and self-shielded isotope-specific one-group cross sections in the target pellets. Spatially dependent heat generation rates were also tallied with MCNP.

Because the targets were irradiated deep within the HFIR PB reflector, variance reduction parameters obtained with the ADVANTG code were used to obtain flux and cross section values with small statistical sampling errors. ORIGEN uses these fluxes and cross sections to compute new isotopic number densities following a short irradiation period of either 1, 3, or 5 days, depending on the time in the HFIR operational cycle. These new target number densities, along with day-specific core and CE number densities from Chandler et al.,[7] were used to generate a new MCNP model. This process was repeated until a full operational cycle consisting of a 26-day irradiation period had been simulated. Following this, a 15-day zero-power decay period was simulated with ORIGEN. The target isotopic number densities from the end of this decay period were combined with BOC core and CE number densities, and another operational cycle was simulated.

III. TARGET DESIGN STUDIES

Previous design studies[2,7] have focused on targets consisting of aluminum-clad cermet pellets. Results from these studies indicate that a maximum PuO_2 production rate of 1.49 kg/yr is achievable. However, this production rate requires the use of all available VXFs in the HFIR PB, assumes a 100% extraction efficiency for the removal of Pu from the cermet pellets, and relies on a VXF-specific irradiation history to yield a ^{238}Pu quality of 85%. Additionally, the process of extracting the Pu from the irradiated targets results in a significant quantity of aluminum-bearing liquid waste.

In an effort to produce more ^{238}Pu with fewer targets and reduce liquid waste during the post-irradiation Pu extraction process, several target designs containing $^{237}NpO_2$ at the highest density that is practically achievable, with no additional filler material, were analyzed. An initial

concept design was based on NpO_2 pellets with an ~0.82 cm diameter stacked into Zircaloy tubing with an arbitrary ~1.00 mm wall thickness. The initial NpO_2 pellet size was similar to that listed for a typical commercial light-water reactor UO_2 fuel pellet.[8]

Once the testing with available equipment proved that $^{237}NpO_2$ pellets of this size could be produced with high enough density to avoid excessive diametral changes during irradiation—typically in a range of 92% ± 2% of TD—several target designs were evaluated. These designs took several factors into consideration, including varying pellet size, target containment form, configuration of fissile material within the targets, orientation of targets within a VXF, movement of targets between cycles, and overall length of irradiation for each target.

III.A. Spectral Effects

An examination of the relevant Np and Pu cross sections[9] indicated the possibility of simultaneously increasing the rate of ^{238}Pu production and reducing the peak heat generated during this process. Table I illustrates that the ^{237}Np capture cross section is higher in the above-thermal or resonance integral (RI) energy range than in the thermal energy range. Conversely, the ^{238}Np fission, ^{238}Pu capture, and ^{239}Pu fission cross sections are higher in the thermal energy range than in the RI range. This leads to the possibility of simultaneously increasing the production of ^{238}Pu and reducing peak heat generation rates by limiting the thermal flux to the target $^{237}NpO_2$ pellets. While the two-group cross sections depicted in Table I are not likely identical to those that would arise from irradiation in any HFIR VXF location, they do at least present the possibility of using spectral shaping to improve ^{238}Pu production rates.

TABLE I. Selected Np and Pu cross sections.

Reaction	Thermal Cross Section (barns)	RI Cross Section (barns)
^{237}Np Capture	150	650
^{238}Np Fission	2100	900
^{238}Pu Capture	540	200
^{239}Pu Fission	750	300

III.B. Self-Shielding Effects

Because of the large capture and fission cross sections involved in the production of ^{238}Pu from ^{237}Np-bearing targets, the spatial variation of the neutron flux and photon flux within the individual pellets comprising the targets will be quite large. To accurately predict the spatial variation of these fluxes and the related heat generation rates and isotopic inventories, the individual pellets must be modeled with significant detail. Figure 3 shows a plan view through the axial centerline of an individual pellet within a target. The pellet is subdivided into 10 radial and 8 azimuthal zones. The flux, isotope-specific one-group capture and fission cross sections, heat generation rates, and isotopic inventories are calculated for each of these 80 depletion zones at each of 10 time-steps for up to 4 HFIR operational cycles. Because each target will consist of multiple locations containing an axial stackup of several dozen pellets, the level of modeling detail shown in Figure 3 is impractical to apply to all pellets in a target.

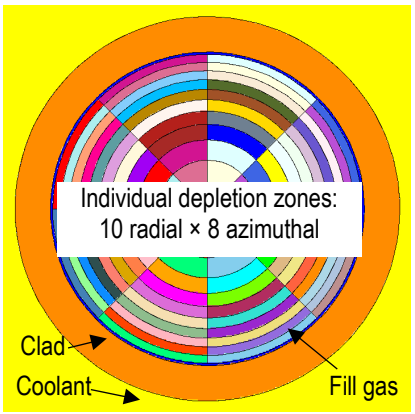

Fig. 3. MCNP model of a single NpO_2 pellet subdivided into 80 unique depletion zones.

Figure 4 presents a plan view through the axial centerline of a target depicting several pellet-bearing pins and a central water-filled aluminum tie rod to connect the above- and below-reflector structure. This figure shows that only a few of the pin locations (pins 1, 3, and 5) contain fully segmented pellets. Because the peak heating rates and ^{238}Pu isotopic production will occur around the horizontal midplane of the HFIR core, the number of fully segmented pellets is further limited to a total of 4 pellets in the axial stackup of pins 1, 3, and 5.

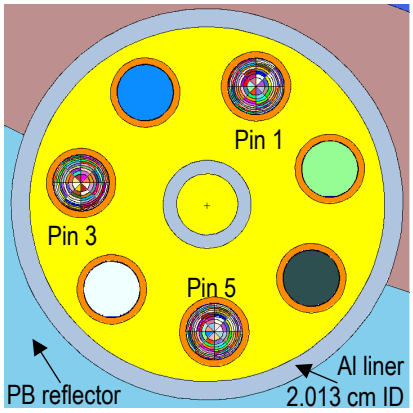

Fig. 4. MCNP model of an open containment target design in a HFIR VXF.

III.C. Design Parameter Variations

Figure 4 presents a specific target configuration out of dozens that were analyzed. The configuration depicted in Figure 4 is typical of open containment designs. In addition

to the open configurations, a set of shielded cassette designs were also considered. Development of these shielded configurations was an attempt to limit the thermal flux impinging on the pellets by (1) minimizing the amount of hydrogenous material in the vicinity of the pellets and (2) placing materials with high thermal neutron absorption cross sections in front of the pellets.

III.C.1 Shielded Cassette Containment Designs

Figure 5 shows a typical shielded cassette containment design configuration. In these configurations, a solid aluminum cassette contains several holes which are intended to contain stacks of pellets, as well as a central flow hole to allow coolant to flow through the assembly. A portion of the cassette is machined away to allow for placement of a thermal neutron shield. A stainless-steel (SS) tube would be used to surround the cassette/shield assembly and provide outer containment to prevent direct contact between the coolant and the shield. In the configuration depicted in Figure 5, a small (2 mm radius) pellet is used. Ultimately, this size of pellet was judged to be problematic from a fabrication standpoint. Larger pellet sizes up to 3.175 mm in radius were analyzed, as were varying shielding materials (Gd, Cd, and BORAL), shielding azimuthal extents (90–360°) and shielding axial extents (±14 through ±26 cm). None of these configurations were able to demonstrate a significant increase in ^{238}Pu production or a significant reduction in peak heat generation rates relative to the best performing open containment designs. This, combined with a more difficult fabrication process, led to the abandonment of the shielded cassette design.

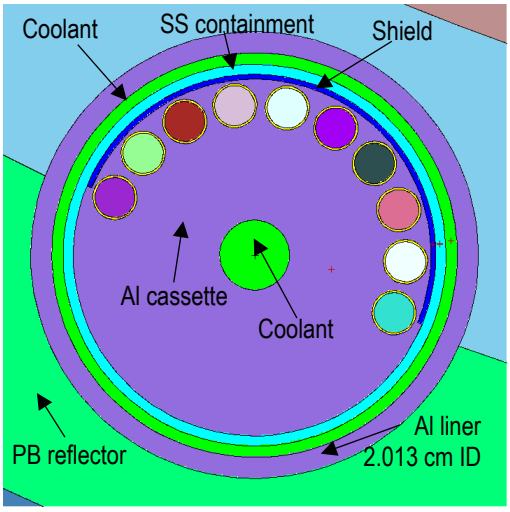

Fig. 5. MCNP model of a typical shielded cassette target design in a HFIR VXF.

In Figure 5, none of the pellets are segmented. Because the shield suppresses the thermal flux so much, the peak heat generation rates will occur just above and just below the axial extent of the shield. To obtain accurate peak heat generation rates, a few pellets in these axial locations were segmented into 80 unique depletion regions consistent with the open containment configurations. These segmented pellets do not appear in the plot presented in Figure 5, which is a slice taken within the axial extent of the notional shield.

III.C.2 Open Containment Designs

The open containment design depicted in Figure 4 shows a configuration of 7 pins. Variations with either 5 or 7 pins were analyzed. The initial 5-pin designs contained pellets with a diameter of ~0.82 cm. Subsequent analyses for the 5- and 7-pin configurations were performed with smaller pellets that had a diameter of ~0.64 cm.

All 5-pin cases analyzed used an arbitrary Zircaloy clad thickness of ~1 mm. The 7-pin cases were analyzed with both Zircaloy and titanium cladding, with each material analyzed for a both a ~1.00 mm wall thickness and a commercially available vendor-specific wall thickness that varied between ~0.63 and ~0.71 mm, depending on the material. Neither of these cladding materials will be dissolved during post-irradiation ^{238}Pu recovery operations, and can therefore be handled as solid waste.

The radial centerlines of all 7 pins depicted in Figure 4 lie on a bolt circle radius (BCR) of 1.45 cm from the radial centerline of the VXF. The 5-pin configurations were analyzed with all 5 pins lying on a BCR between ~1.12 and 1.35 cm. The 7-pin configurations were analyzed for BCRs between ~1.12 and 1.45 cm.

Irradiation histories of either 3 or 4 HFIR operational cycles with rotation of the targets between cycles and potential movement of the targets from inner to outer VXF locations were considered. For targets irradiated for only 3 cycles, an ~103° rotation after each cycle was modeled. For targets irradiated for 4 cycles, an ~154° counterclockwise rotation between cycles 1 and 2 and a subsequent ~154° clockwise rotation between cycles 2 and 3 were modeled. These targets were not rotated after cycle three because they were moved to a lower flux outer VXF location after the second cycle. These rotations ensure that a single pin will be located in the worst-case configuration, thus yielding a conservative prediction for the peak heat generation rate. However, the rotations will ensure that no pin is facing the core for the entire irradiation history. This reduces overall peak heat generation rates and increases ^{238}Pu production by exposing relatively fresher fuel to the higher fluxes experienced on the front of the targets.

IV. RESULTS

To demonstrate the high degree of self-shielding discussed in previous sections, Figure 6 presents a typical heat generation rate profile in a $^{237}NpO_2$ pellet at the worst time in life. This figure clearly illustrates that the heat generation rates are predominantly a surface effect, and the rates diminish rapidly with distance into the pellet. The

peak heat generation rate on the surface is ~390 W/g. This drops to ~23 W/g near the center of the pellet. The peak heat generation rates for all open containment configurations analyzed vary between ~290–435 W/g for the worst-case pellet in a given target.

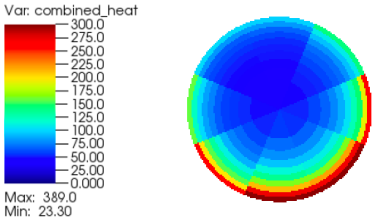

Fig. 6. Typical heat generation rate profile for an NpO_2 pellet irradiated for multiple cycles in a HFIR VXF.

IV.A. Preliminary Production Assessments

By placing a minimum of 3 $^{237}NpO_2$-bearing targets into various VXF locations in HFIR at the beginning of each of 7 operational cycles per year and performing the rotations and movements described in the previous section, a steady-state condition of at least 12 targets being irradiated and 3 targets being removed after each cycle will be achieved after a start-up period of just 4 cycles. Current predictions show that, with this operational tempo, over the course of 7 cycles per year, between ~1.05 and ~1.32 kg of ^{238}Pu (~1.25-1.58 kg PuO_2) could be generated, depending on target configuration. Furthermore, the ^{238}Pu quality is predicted to be between ~94 and ~95%. By downblending this with Pu of a lower quality and converting the Pu into oxide, a PuO_2 production rate of 1.5 kg per year may be achievable, subject to additional computational validation and operational constraints, as described below.

IV.B. Additional Considerations

The results presented in the paper are preliminary. Final documentation and internal reviews must be completed before any of the target design variants can be fabricated and irradiated in HFIR. Irradiation of 4 previously approved test target designs, containing only 4 $^{237}NpO_2$ pellets each, have taken place. Results from the post-irradiation examination (PIE) of these test targets will be used to help benchmark the current calculations.

HFIR is a multi-mission facility. As such, multiple operational constraints must be considered. Preliminary, undocumented internal analyses indicate that the current target designs will likely not exceed the maximum allowable cycle length (12 hours) or beam tube flux (5%) reductions. These analyses must still be documented and reviewed.

Additional steady-state and transient thermal-hydraulic analyses, as well as studies to quantify instrumentation effects must still be performed, documented, and reviewed.

V. CONCLUSIONS

Various NpO_2 target configurations and irradiation histories have been analyzed. Preliminary predictions indicate that ~1.5 kg/year of PuO_2 with a ^{238}Pu quality of 85% could be met using 12 VXF locations if seven 26-day irradiation cycles per year can be maintained. Additional calculations and planned PIE of previously irradiated test targets are needed to confirm the preliminary calculations presented in his paper.

ACKNOWLEDGMENTS

The authors would like to acknowledge the support for the work provided by NASA's Science Mission Directorate and the US DOE Office of Nuclear Infrastructure Programs. The authors would also like to thank David Chandler and Stephen Wilson of ORNL for their reviews of this paper.

REFERENCES

1. R. M. WHAM et al., "The Plutonium-238 Supply Project," *The 19th Pacific Basin Nuclear Conference*, Vancouver, British Columbia, Canada (2014).
2. D. CHANDLER and R. J. ELLIS, "Neutronics Simulations of ^{237}Np Targets to Support Safety-Basis and ^{238}Pu Production Assessment Efforts at the High Flux Isotope Reactor," *Proc. NETS 2015*, Albuquerque, NM (2015).
3. R. D. CHEVERTON and T. M. SIMS, "HFIR Core Nuclear Design," ORNL-4621, Oak Ridge National Laboratory (1971).
4. X-5 Monte Carlo Team, "MCNP – A General Monte Carlo N-Particle Transport Code, Version 5. Volume I: Overview and Theory," LA-UR-03-1987, Los Alamos National Laboratory (2003).
5. S. W. MOSHER et al., "ADVANTG – An Automated Variance Reduction Parameter Generator," ORNL/TM-2013/416 Rev. 1, Oak Ridge National Laboratory (2015).
6. "SCALE: A Comprehensive Modeling and Simulation Suite for Nuclear Safety Analysis and Design," ORNL/TM-2005/39, Version 6.1, Oak Ridge National Laboratory (2011).
7. D. CHANDLER, and R. J. Ellis, "Development of an Efficient Approach to Perform Neutronics Simulations for Plutonium-238 Production," *Proc. PHYSOR 2016*, Sun Valley, ID (2016).
8. J. J. DUDERSTADT and L. J. HAMILTON, Nuclear Reactor Analysis, p. 635, John Wiley & Sons, New York, NY (1976).
9. E. M. BAUM, H. D. KNOX and T. R. MILLER, *Nuclides and Isotopes, Chart of the Nuclides – 16th edition*, p.70, KAPL, Inc., Schenectady, NY (2002).